CHEMICAL AND PHYSICAL QUENCHING OF THE E(O⁺) ION-PAIR STATE OF IBr BY THE NOBLE GASES

JEREMY P. T. WILKINSON, MICHAEL MACDONALD and ROBERT J. DONOVAN

Department of Chemistry, University of Edinburgh, West Mains Road, Edinburgh EH9 3JJ (U.K.)

(Received April 28, 1986)

Summary

Absolute rate data for the quenching of IBr(EO⁺) by helium, argon and xenon are presented ($k_{He} = (3.3 \pm 0.6) \times 10^{-10}$ cm^3 molecule^{-1} s^{-1}, $k_{Ar} = (4.4 \pm 0.3) \times 10^{-10}$ cm^3 molecule^{-1} s^{-1} and $k_{Xe} = (2.7 \pm 0.4) \times 10^{-10}$ cm^3 molecule^{-1} s^{-1}). With helium and argon, physical quenching involving efficient interstate transfer to the D$'($$^3\Pi_2$) state is observed. Quenching by xenon occurs by both physical and chemical channels: the chemical channel leads to formation of electronically excited XeBr(B $^2\Sigma$) which is observed in fluorescence at 280 nm, while the physical channel populates the D$'($$^3\Pi_2$) state. The threshold wavelength for formation of excited XeBr(B $^2\Sigma$) is determined as $\lambda = 198.5 \pm 1.0$ nm.

1. Introduction

We have previously shown [1] that excitation of IBr at 193 nm (ArF laser), in the presence of xenon, leads to the formation of electronically excited XeBr(B $^2\Sigma$). It was suggested that IBr is initially excited to a low lying ion-pair state and that this state undergoes efficient reaction with xenon atoms to produce XeBr(B $^2\Sigma$). The excited XeBr product was observed in fluorescence at 280 nm.

In this paper we report a more detailed study using a fluorometer which allows the excitation wavelength to be tuned from 188 nm to longer wavelengths and have thereby determined the threshold for the process

$$IBr(EO^+) + Xe \longrightarrow XeBr(B\ ^2\Sigma) + I$$

We also report studies of the physical quenching of IBr(EO⁺) by the noble gases helium and argon. (The nomenclature used for the ion-pair states of IBr has not been entirely consistent. We have followed the nomenclature used by Brand *et al.* [2] and designate the lowest O⁺ state of IBr as the E state.)

2. Experimental details

The spectrofluorometer employed for this work was a Perkin–Elmer model 650-40. This consists of a pair of $f/3$ monochromators mounted at right angles, one acting as a wavelength selector for the excitation beam with the other resolving fluorescence from the sample. The excitation monochromator, the grating of which was blazed at 300 nm, was used to select the desired wavelength from the output of a 150 W xenon lamp. The bandwidth of this monochromator was continuously variable between 1.5 and 20 nm. The excitation beam was then passed through a 1 cm × 1 cm square cross-section quartz fluorescence cell of standard design (Thermal Syndicate Ltd.), which was fitted with a greaseless tap. Fluorescence was then collected at right angles to the excitation beam, via the second $f/3$ monochromator, again with a variable bandpass of 1.5 to 20 nm but with a grating blazed at 450 nm; signals were detected using a Hamamatsu R928 photomultiplier. The two monochromators were controlled by a dedicated microprocessor system.

The spectrofluorometer was used in two different modes. The first mode was that for fluorescence emission spectroscopy, where the excitation radiation is held at a constant wavelength and bandwidth and the emission monochromator is scanned. This yields a spectrum of the fluorescence produced by excitation at a given fixed wavelength. The second mode used was fluorescence excitation spectroscopy, wherein the excitation wavelength is scanned whilst the emission wavelength is held constant, usually at a wavelength corresponding to an intense feature in the fluorescence spectrum. The excitation spectra thus obtained are directly analogous to the excitation spectra which are obtained by laser-induced fluorescence, and are related to the absorption spectrum of the molecule under study.

The microcomputer program allows the wavelengths of both the emission and excitation monochromators to be set to any value between 200 and 800 nm. However, since absorption by IBr at 200 nm is weak and as the absorption coefficient increases rapidly below this wavelength, we ideally require excitation wavelengths lower than 200 nm. This was achieved in two ways. The first method used was to set the excitation monochromator to its low wavelength limit at 200 nm and to open up the bandpass to its maximum value (20 nm) which leads to irradiation of the sample at wavelengths below 200 nm. This method is limited in its applications since the excitation wavelength is poorly characterized and not tunable; however, in studies of the collisional quenching of $IBr(EO^+)$ the relatively large signal intensities more than compensate for this disadvantage.

The second method used, which allowed the excitation wavelength to be tuned, took advantage of the fact that excitation of IBr with radiation of wavelengths around 380 - 400 nm does not give rise to any detectable visible or UV fluorescence. Thus, by using the excitation monochromator in second order, excitation wavelengths in the region 180 - 200 nm could be obtained by scanning the monochromator through the (first order) region between 360 and 400 nm. The only disadvantage of this method was that

some regions of the fluorescence from IBr were obscured (*i.e.* 360 - 400 nm) by scattered first-order light.

The samples of IBr, together with any quenching gases, were introduced into the cell using a standard greaseless vacuum line. They were allowed to mix by diffusion by leaving samples to stand for periods of 20 - 30 min and thorough mixing was confirmed by repeated measurement of the fluorescence signal until a constant value was reached. The IBr samples were taken from the vapour above solid IBr which was prepared by reacting equimolar amounts of iodine and bromine. The IBr samples were then diluted by the addition of an approximately equal pressure of pure bromine, in order to suppress the I_2 which exists in equilibrium with IBr. This small amount of bromine has little effect upon the fluorescence measurements, merely changing the measured intensities by a constant small amount, since absorption by Br_2 is negligible at the wavelengths used here.

3. Results and discussion

The dispersed fluorescence from IBr, excited at 200 nm, is shown in Fig. 1. The spectrum consists of two oscillatory continua that are character-
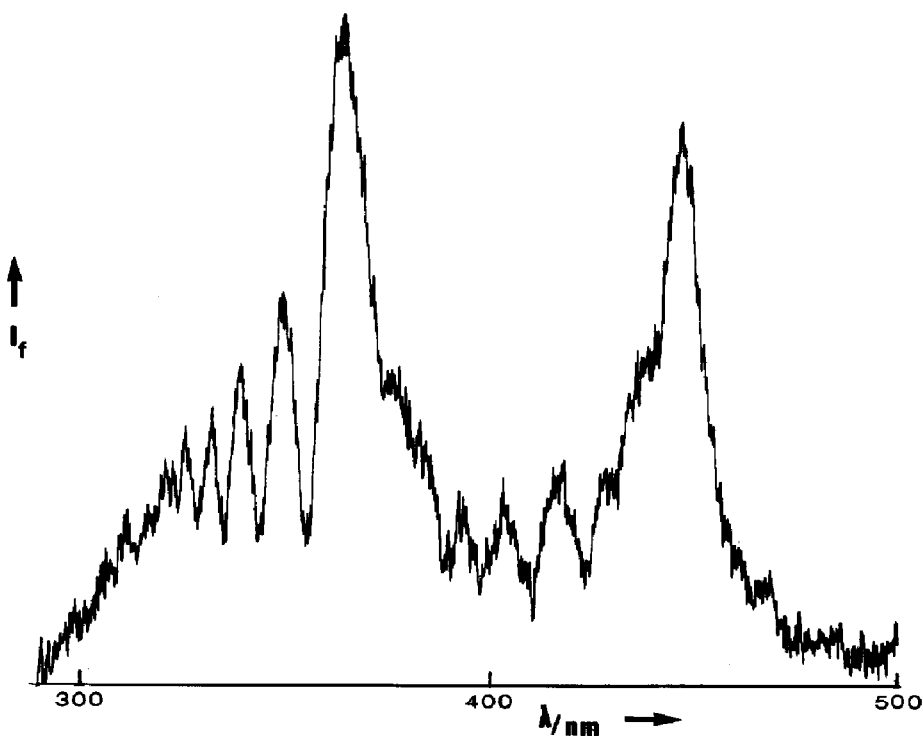

Fig. 1. Fluorescence from $IBr(EO^+)$, following excitation at 200 nm ($\Delta\lambda = 15$ nm), showing the presence of two oscillatory continuum systems. The spectrum extends below 300 nm, although it is curtailed here by the presence of a cut-off filter: the spectrum was recorded with a bandwidth of 3 nm ($P_{IBr} = P_{Br_2} = 170$ N m^{-2}).

istic of fluorescence from high vibrational levels of ion-pair states. The lowest ion-pair state to which a transition from the ground electronic state $X(O^+)$ is allowed is the $E(O^+)$ state [2]. The $E(O^+)$ state is therefore assigned as the upper state responsible for the oscillatory continua shown in Fig. 1. A full analysis of these oscillatory continua will be given elsewhere. The strong Rydberg system which dominates the absorption spectrum in the region 186 - 197 nm is strongly predissociated [3] and is thus not observed in fluorescence.

Addition of argon quenches the fluorescence shown in Fig. 1 and this is replaced by a strong transition centred at 385 nm (see Fig. 2). This is readily identified as the $D'(^3\Pi_2) \to A'(^3\Pi_2)$ transition of IBr. Thus, quenching of IBr resembles that of I_2 and Br_2 [4, 5] in that the initially populated ion-pair state undergoes rapid cascading within the ion-pair manifold, leading to a build-up of population in the low vibrational levels of the lowest ion-pair state (*i.e.* the D' state).
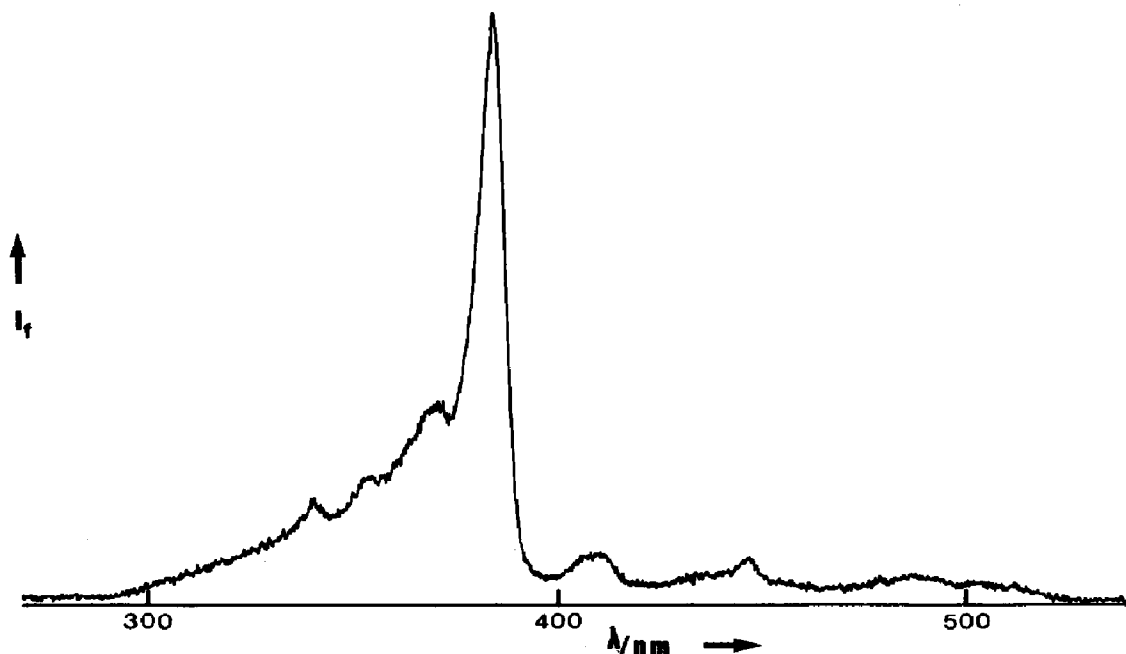

Fig. 2. Fluorescence from IBr ($D'\,^3\Pi_2 \to A'\,^3\Pi_2$) following interstate transfer by collisions with argon ($P_{IBr} = 160$ N m^{-2}; $P_{Br_2} = 150$ N m^{-2}; $P_{Ar} = 7.45$ kN m^{-2}).

Quenching of the $E(O^+)$ state of IBr by argon was studied by monitoring the $E \to X$ fluorescence at 445 nm. A Stern–Volmer plot of the data is shown in Fig. 3. The slope of this plot combined with the previously reported [6] lifetime data for IBr $E(O^+)$, under the conditions used here, yields a quenching rate constant for argon of $(4.4 \pm 0.3) \times 10^{-10}$ cm^3 molecule^{-1} s^{-1}. Quenching by helium was also examined using the same procedure and a quenching rate constant of $(3.3 \pm 0.6) \times 10^{-10}$ cm^3 molecule^{-1} s^{-1} was obtained.

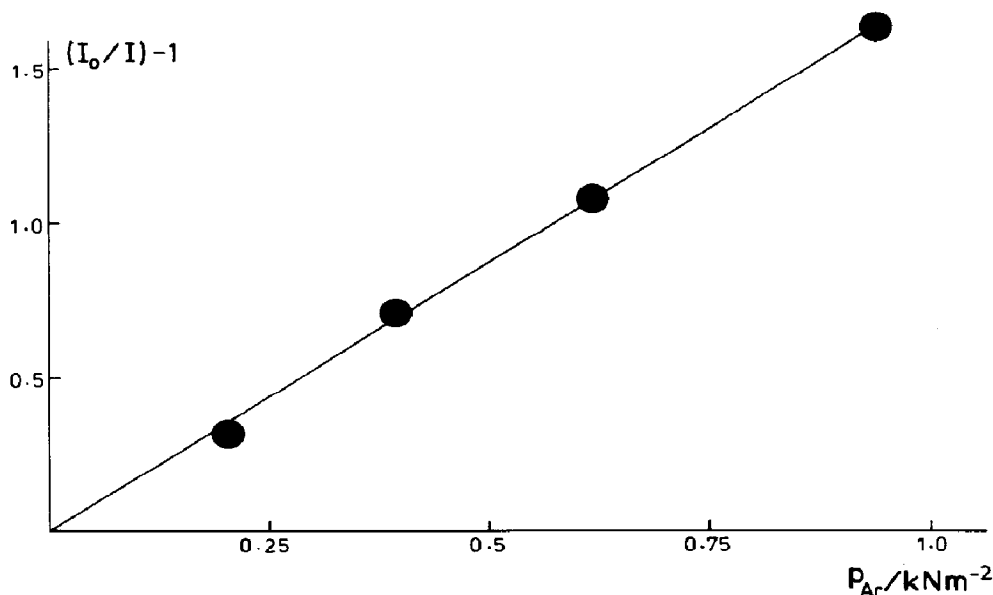Fig. 3. Plot of the reciprocal fluorescence intensity from $IBr(EO^+)$ at $\lambda = 445$ nm against pressure of argon ($P_{IBr} = P_{Br_2} = 150$ N m^{-2}).

The high efficiency for quenching by helium is particularly interesting as momentum transfer is very unfavourable in this case. The key to an understanding of this behaviour lies in the presence of a high density of states, owing to the close proximity of several ion-pair states and the high density of rovibronic levels within each of these states. A strong interaction between the polar ion-pair state and the colliding atom is expected, as there is theoretical evidence for a substantially bound ($\Delta E \approx 1.5$ eV) complex for the analogous system involving helium and the ion-pair state of H_2 [7]. A strong interaction of this type could lead to efficient coupling between electronic and nuclear degrees of freedom and we therefore suggest that collision of $IBr(EO^+)$ with helium (and argon) leads to the transfer of substantial amounts of energy into internal motion of IBr and kinetic energy of the departing noble gas atom.

Quenching of $IBr(EO^+)$ by xenon produces an additional strong emission band at 280 nm (see Fig. 4) which is readily assigned to $XeBr(B\ ^2\Sigma \rightarrow X\ ^2\Sigma)$. The threshold for formation of $XeBr(B\ ^2\Sigma)$ was determined by scanning the excitation monochromator while keeping the fluorescence monochromator fixed at 280 nm. The resulting excitation spectrum is shown in Fig. 5. The broad structure superimposed on the excitation function is due to absorption by O_2 (i.e. Schuman–Runge absorption). The lower line in Fig. 5 shows the fluorescence signal at 290 nm, adjacent to the $XeBr(B\ ^2\Sigma \rightarrow X\ ^2\Sigma)$ band; the signal at 280 nm must also contain a small contribution from $IBr(EO^+ \rightarrow XO^+)$ (the signals from $IBr(EO^+)$ at 280 nm and 290 nm are approximately the same).
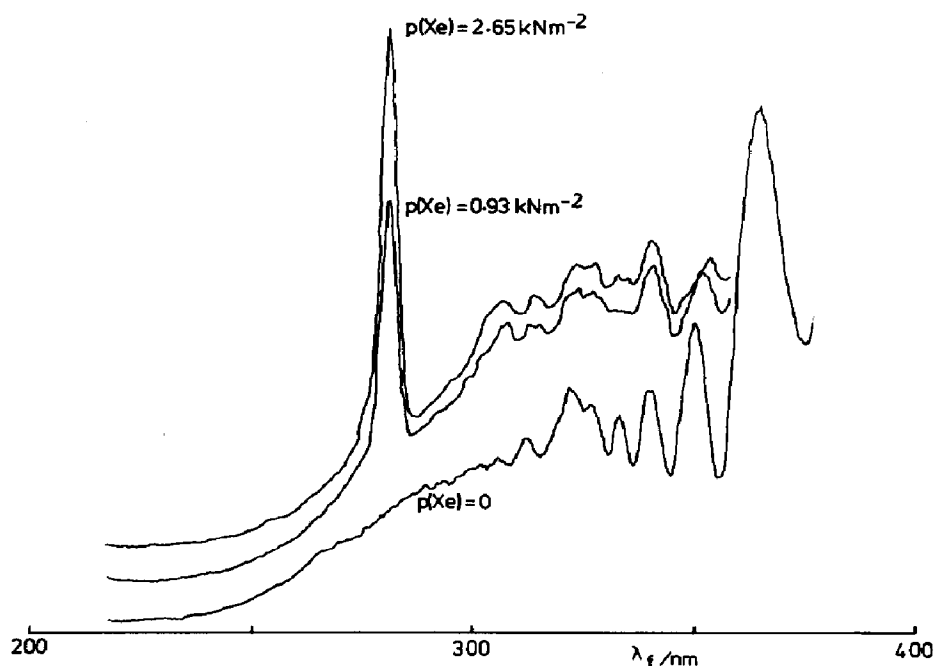
Fig. 4. Fluorescence from IBr–Xe mixtures, showing the XeBr (B $^2\Sigma \rightarrow$ X $^2\Sigma$) system at 280 nm (P_{IBr} = 170 N m^{-2}; P_{Br_2} = 170 N m^{-2}; P_{Xe} as shown).

Taking account of the bandwidth (1 nm) of the excitation monochromator, the threshold for formation of XeBr(B $^2\Sigma$) was determined as 198.5 ± 1.0 nm (50 380 ± 250 cm^{-1}). The observed threshold is thus equal to the thermodynamic threshold of 50 330 cm^{-1} [8].

It is clear that both physical and chemical quenching channels compete in the removal of IBr(EO$^+$) and in the future we propose to study this competition in more detail using tunable synchrotron radiation. This will enable us to cover a wider energy range than that available with the commercial fluorometer employed for this work.

The rate constant for total removal of IBr(EO$^+$) by xenon was measured by the method described above for argon and is given in Table 1.

TABLE 1

Absolute rate data for quenching of IBr(EO$^+$) by the noble gases helium, argon and xenon

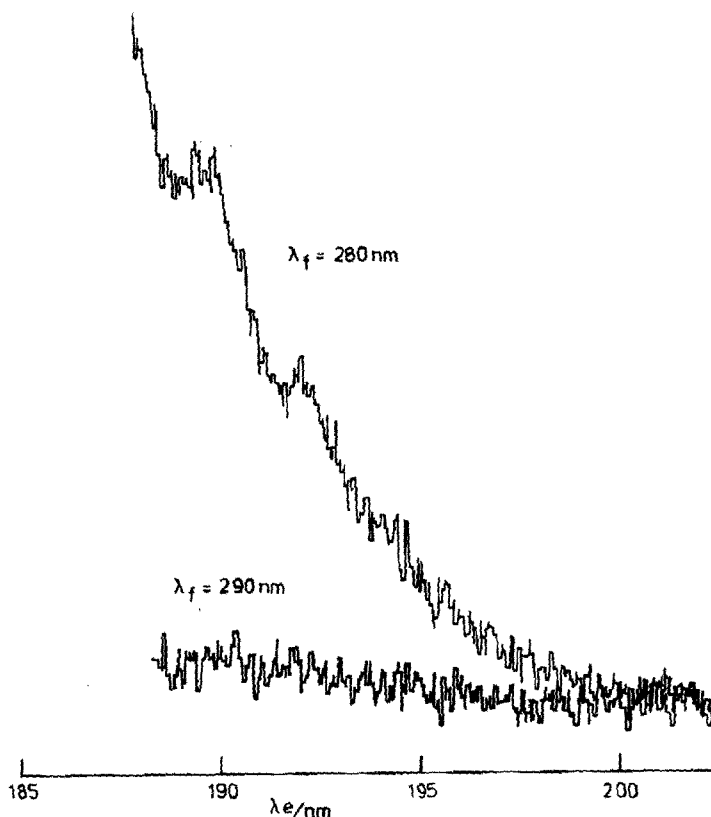| Quenching gas	Quenching rate constant k (cm^3 molecule^{-1} s^{-1})	Cross-section σ (Å^2)
He	$(3.3 \pm 0.6) \times 10^{-10}$	26 ± 5
Ar	$(4.4 \pm 0.3) \times 10^{-10}$	101 ± 7
Xe	$(2.7 \pm 0.4) \times 10^{-10}$	96 ± 15

Fig. 5. Excitation function for XeBr(B $^2\Sigma$) formation in the reaction between IBr(EO$^+$) and xenon. The lower trace shows the background fluorescence at 290 nm, adjacent to the XeBr(B $^2\Sigma \rightarrow$ X $^2\Sigma$) system ($P_{IBr} = P_{Br_2} = 150$ N m^{-2}; $P_{Xe} = 12$ kN m^{-2}).

4. Mechanism for reaction with xenon

It is now well established that the reaction between the heavier excited metastable noble gas atoms (argon, krypton and xenon) and halogen molecules, to produce the products AX* + X, proceeds via an electron jump (harpoon) mechanism, in which the reactants are transferred from the initial covalent surface to an ionic surface, correlating with A$^+$ and X$_2^-$; this ionic surface then leads directly to the products [9, 10]. Collision between X$_2^*$ and A must also occur initially on a covalent surface which lies somewhat below that for A* and X$_2$. The X$_2^*$ + A surface is therefore expected to cross the ionic surface at slightly shorter internuclear separation compared with the A* + X$_2$ crossing. Thus, the reactants X$_2^*$ + A can transfer to the ionic surface at this crossing and reaction to form AX* + X will ensue. However, the electronic rearrangement required is clearly more complicated in this case and involves, at least, a two-electron process. The large total cross-sections observed for quenching of IBr(EO$^+$) by the noble gases (Table 1)

support our proposal that an electron transfer mechanism is involved, but one might have expected the cross-section for xenon to be greater than that for argon, owing to the larger crossing radius for xenon (resulting from the lower ionization energy). However, the efficiency for transfer to the ionic surface could differ in the two cases and our results suggest that the efficiency of electron transfer with xenon is slightly lower than that for argon. This is a reasonable conclusion, as the efficiency for electron transfer, in similar and more thoroughly established collision systems [11], is known to show a strong dependence on the position of the crossing point and to decline to zero at large crossing distances. This type of reaction deserves more detailed theoretical consideration and we hope that the present report will stimulate such work.

5. Conclusions

The $E(O^+)$ state of IBr undergoes very efficient interstate transfer (close to the gas kinetic collision rate) on collision with the noble gases helium, argon and xenon. Rapid cascading occurs to low vibrational levels of the lowest ion-pair state (the D' state), which is itself very resistant to further quenching. The high efficiency of interstate transfer suggests that a strong interaction takes place between the collision partners and that a large amount of the available energy is partitioned into internal and translational motion of the products. Quenching by xenon also produces $XeBr(B\ ^2\Sigma)$ and a mechanism involving transfer to an ionic surface is proposed. This same mechanism is also probably involved in interstate transfer. The observed threshold ($50\,380 \pm 250\ cm^{-1}$) for formation of $XeBr(B\ ^2\Sigma)$ is equal to the thermodynamic threshold ($50\,330\ cm^{-1}$).

Acknowledgments

References

1 J. P. T. Wilkinson, M. MacDonald and R. J. Donovan, *Chem. Phys. Lett., 101* (1983) 284.
2 J. C. D. Brand, U. D. Deshpande, A. R. Hoy, S. M. Jaywant and E. J. Woods, *J. Mol. Spectrosc., 99* (1983) 339.
3 R. J. Donovan and N. Nishi, *Chem. Phys. Lett., 117* (1985) 286.
4 M. J. Shaw, C. B. Edwards, F. O'Neill, C. Fotakis and R. J. Donovan, *Appl. Phys. Lett., 37* (1980) 346.

5   M. MacDonald, R. J. Donovan and M. C. Gower, *Chem. Phys. Lett., 97* (1983) 72.
6   R. J. Donovan, G. Gilbert, M. MacDonald, J. P. T. Wilkinson, I. Munro and D. Shaw, *J. Photochem., 31* (1985) 1.
7   C. A. Nicolaides and A. Zdetsis, *J. Chem. Phys., 80* (1984) 1900.
8   G. Herzberg and K. P. Huber, *Constants of Diatomic Molecules*, Van Nostrand Reinhold, New York, 1979, p. 336.
9   M. F. Golde and B. A. Thrush, *Chem. Phys. Lett., 29* (1974) 486.
10 J. E. Velazco and D. W. Setser, *J. Chem. Phys., 62* (1975) 1990.
11 R. B. Bernstein, *Classical Dynamics via Molecular Beam and Laser Techniques*, Clarendon Press, 1982, Chapter 8.